ELSEVIER

Bonding in hydrogenated diamond-like carbon by Raman spectroscopy

C. Casiraghi[a], F. Piazza[a], A.C. Ferrari[a,*], D. Grambole[b], J. Robertson[a]

[a]*Department of Engineering, University of Cambridge, Trumpington Street, Cambridge CB2 1PZ, UK*
[b]*Forschungszentrum Rossendorf, Institut für Ionenstrahlphysik und Materialforschung, Dresden, Germany*

Abstract

We study the 514 and 244 nm Raman spectra of a wide variety of hydrogenated amorphous carbons (a-C:H). The hydrogen content can be estimated from the slope of the photoluminescence background (PL) of the spectra measured at 514.5 nm. Generally, the evolution of the sp^2 and sp^3 phases is not independent for as-deposited a-C:H samples. This, in principle, allows us to derive their structural and optical properties just by studying the visible Raman spectra. For highly hydrogenated samples, the PL background overshadows the visible Raman spectra, and UV excitation is the only way to measure a Raman spectrum.
© 2005 Elsevier B.V. All rights reserved.

Keywords: Hydrogenated amorphous carbon; Raman spectroscopy; Optical properties; Mechanical properties

1. Introduction

Diamond-like carbon (DLC) is an amorphous carbon with a significant fraction of C-C sp^3 bonds. Tetrahedral amorphous carbon (ta-C) is the DLC with the maximum sp^3 content. We classify hydrogenated amorphous carbons into four classes:

(1) a-C:H films with the highest H content (40–50%). These films can have up to ~60% sp^3. However, most of the sp^3 bonds are hydrogen terminated, and this material is soft and with low density. We call these films polymer-like a-C:H (PLCH). Their band gap is above 2 eV and can reach 4 eV [1].

(2) a-C:H films with intermediate H content (20–40%). Even if these films have a lower overall sp^3 content, they have more C-C sp^3 bonds compared to PLCH. Thus, they have better mechanical properties. Their optical gap is between 1 and 2 eV [1]. We call these films diamond-like a-C:H (DLCH).

(3) Hydrogenated tetrahedral amorphous carbon films (ta-C:H). ta-C:H films are a class of DLCH for which the C-C sp^3 content can be increased whilst keeping a fixed H content. Thus, most films defined in literature as ta-C:H are just DLCHs. However, the ta-C:H films with the highest sp^3 content (~70%) and ~25 at.% H content do really fall in a different category as also shown by their Raman spectra, their higher density (up to 2.4 g/cm³) and Young's Modulus (up to 300 GPa) [2,3]. The optical gap can reach 2.3 eV [4].

(4) a-C:H with low H content (less than 20%). They have a high sp^2 content and sp^2 clustering. The gap is under 1 eV [1]. We call these films graphite-like a-C:H (GLCH).

Raman spectroscopy is a fast and nondestructive tool for characterisation of amorphous carbons. All carbons show common features in their Raman spectra in the 800–2000 cm⁻¹ region, the so-called G and D peaks, which lie at around 1560 and 1360 cm⁻¹, respectively, for visible excitation, and the T peak at around 1060 cm⁻¹, which becomes visible only for UV excitation [5,6]. The G peak is due to the bond stretching of all pairs of sp^2 atoms in both rings and chains. The D peak is due to the breathing modes of sp^2 atoms in rings [5,7]. The T peak is due to the C–C sp^3 vibrations [6].

In previous papers, we have shown that multiwavelength Raman spectra can be used to distinguish the different types of amorphous carbons and to assess their structural and the

---

mechanical properties. We discussed hydrogen-free amorphous carbons in Ref. [5,6] and amorphous carbon nitrides in Refs. [10,11]. We dealt with nanodiamond in Ref. [12]. In this paper, we present a detailed study of the Raman spectra of hydrogenated amorphous carbons.

Within the three-stage model of the Raman spectra of carbon films [5,6,10], the evolution of the Raman spectra is understood by considering an amorphisation trajectory, starting from perfect graphite. The main factor affecting peaks position, width, and intensity is the clustering of the sp^2 phase. The sp^2 clustering can in principle vary independently from the sp^3 content, so that for a given sp^3 content and excitation energy, we can have a number of different Raman spectra, or, equivalently, similar Raman spectra for different sp^3 contents. For UV excitation, an increase in clustering always lowers the G peak position. If two samples have similar G peak positions in visible Raman but different ones in UV Raman, the sample with the lower G position in the UV has higher sp^2 clustering. A multiwavelength Raman analysis is thus important to fully characterise the samples. A very useful parameter is then the G peak dispersion (Gdisp). This is defined as the slope of the line connecting the G peak positions, measured at different excitation wavelengths. Another useful parameter to monitor the carbon bonding is the full-width at half maximum of the G peak ($FWHM_G$). Both $FWHM_G$ and Gdisp always increase as the disorder increases, at every excitation wavelength [6,10,11].

Contrary to the introduction of nitrogen or to the effect of annealing [10,5,6], the introduction of hydrogen into an amorphous carbon links the amount and configuration of the sp^2 phase with the sp^3 content. In principle, this is quite fortunate, since it implies that for a-C:H, a single wavelength Raman study can be enough to quantify the H and sp^3 content, the optical and mechanical properties. Here we show that this indeed can be the case. However, we urge extreme caution when doing a single wavelength analysis, since some deposition processes can introduce sp^2 clusters even in samples with high H content [13]. In these cases, a multiwavelength Raman spectroscopy is necessary to extract reliable information.

Due to the overwhelming cross-section of the sp^2 carbon phase for visible excitation, the C–H stretching modes can only be seen for UV excitation [6]. However, a typical signature of hydrogenated samples in visible Raman is the increasing photoluminescence background (PL) for increasing H content. This is due to the hydrogen saturation of nonradiative recombination centres [8]. For H content over ~40–45%, this background usually overshadows the Raman signal of a-C:H [5,6,9]. The ratio between the slope, m, of the fitted linear background and the intensity of the G peak, $m/I(G)$, can be empirically used as a measure of the bonded H content, as will be shown in Section 3.

2. Experimental

We grew more than 50 hydrogenated carbon films by using different deposition systems: a 13.56 MHz rf plasma-enhanced chemical vapour deposition (PECVD) system and an electron cyclotron wave resonance (ECWR) source [4]. We also studied the Raman spectra of a-C:H films deposited
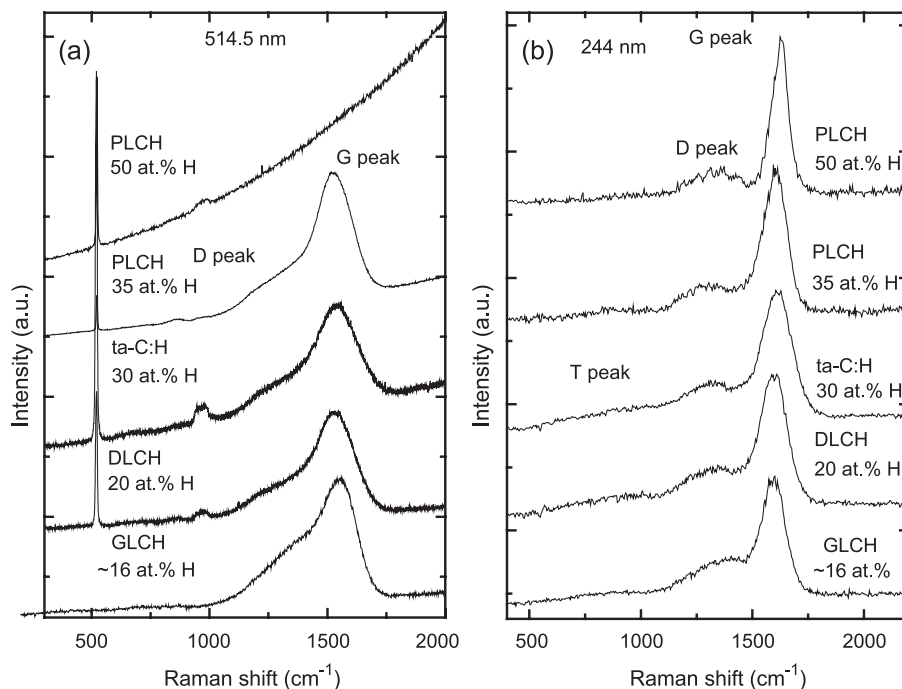

Fig. 1. Raman spectra of template a-C:H films at (a) 514.5 and (b) 244 nm.

by a distributed electron cyclotron resonance (DECR) plasma reactor [14]. We considered the effect of two precursors gases (CH_4 and C_2H_2). All the samples were deposited simultaneously on silicon (for Raman measurements) and on quartz (for optical gap measurements). The optical gap (Tauc and E_{04}) was derived by UV–Visible Spectroscopy. The hydrogen content and density of the samples were determined from nuclear reaction analysis (NRA). The Young's modulus (E) was derived by the laser acoustic waves technique or by surface Brillouin scattering [3,15]. We also compared the measurements on our films with data in literature [16,17].

Unpolarized Raman spectra were acquired at 244 and 514.5 nm excitations using two Renishaw micro-Raman 1000 spectrometer optimised for UV and visible excitations, respectively. The UV Raman spectra were collected with a $40\times$ objective and a UV-enhanced charge-coupled device camera. The spectral resolution was ~6 cm^{-1}. Hydrogenated carbons films are particularly sensitive to UV excitation and can be easily damaged. In order to avoid damage, the power on the sample was kept well below 1 mW (down to 0.005 mW), and samples were placed on a spinner rotating at high speed (>3000 rpm). These procedures ensure no visible damage is produced on the sample surface and no change of the spectral shape during the measurements. The visible Raman spectra were collected with a $100\times$ objective. The spectra resolution was 1 cm^{-1}. The power on the samples was always kept below 4 mW (down to 0.4 mW) to avoid damage. Since here we never compare the absolute intensities of the measured spectra, the acquisition time and power on the sample are changed in order to get the least noisy spectrum with no sample damage.

In this paper the spectra are fitted with Gaussians for the G and D peaks. The PL background has been calculated as the ratio between the slope m of the spectra, measured between 1050 and 1800 cm^{-1}, and the intensity (i.e., the height) of the G peak and is measured in microns. The Gaussian fit is used in order to facilitate the comparison with other data present in literature. It is also better than the Breit–Wigner–Fano (BWF) fit to avoid problems in the determination of the PL background slope.

3. Results and discussions

Fig. 1a,b show the 514.5 and 244 nm Raman spectra measured on some template a-C:H films. Note that for low H, the spectra do not exhibit a PL background, whilst for the maximum H concentration (45–50%), the PL is so strong that the spectrum is featureless. On the contrary, the UV Raman spectrum can always be measured, irrespective of the H content. Indeed, UV Raman spectra showing two well-separated features (such as the top spectra in Fig. 1b) are an unambiguous signature of PLCH films [6].

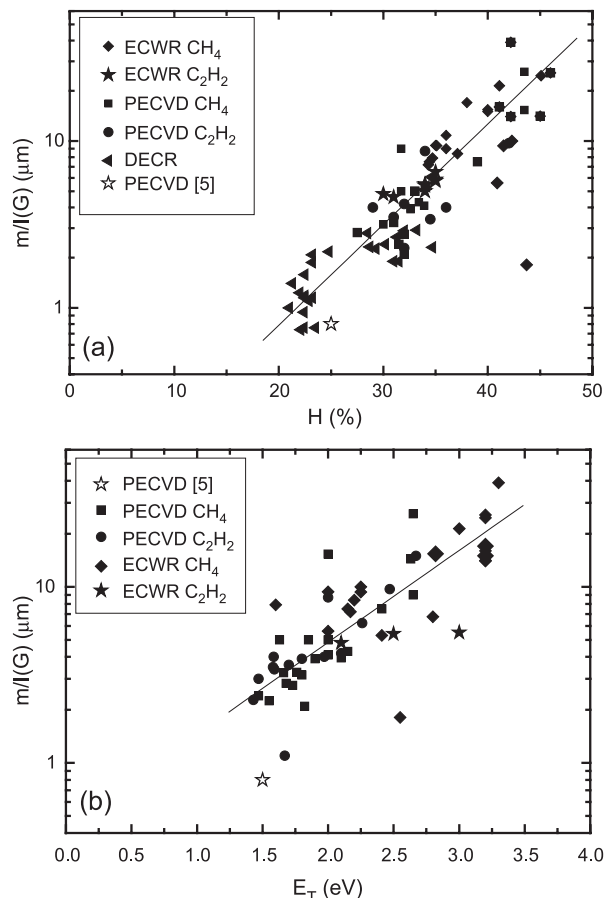Fig. 2a shows that the PL background, $m/I(G)$, increases exponentially with the hydrogen content, for any

Fig. 2. PL slope background $m/I(G)$, as a function of (a) H content and (b) Tauc gap. The lines are fit to the data. Note that for H<20 at.%, the spectra do not show PL. For H>45 at.%, the spectra become featureless, so $I(G)$ cannot be properly defined.

film we examined. From Fig. 2a, we can get a simple formula, which allows a qualitative assessment of the hydrogen content:

$$H\ [at\%] = 21.7 + 16.6 \log \left\{ \frac{m}{I(G)}[\mu m] \right\} \qquad (1)$$

Fig. 2b shows that $m/I(G)$ also increases exponentially with the Tauc gap. Note that our samples can have Tauc gap bigger than 2.4 eV, but we are always exciting at 2.4 eV. By doing so, we only probe the radiative recombination efficiency of subband gap clusters. This, anyway, allows an estimate of the H content, because the recombination efficiency of subband gap clusters increases as well with the amount of hydrogen [1].

Fig. 2a,b also implies that H and gap are proportional. This is directly shown in Fig. 3. By fitting the data in Fig. 3, we get a simple formula relating H and Tauc gap for 20 at.%<H<50 at.% :

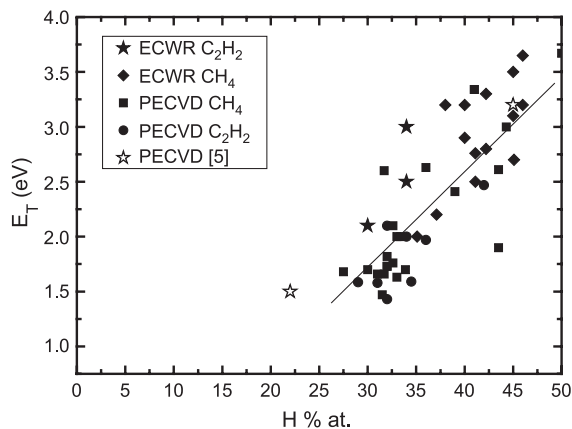$$E_T[eV] = -0.9 + 0.09 \times H[at.\%] \qquad (2)$$
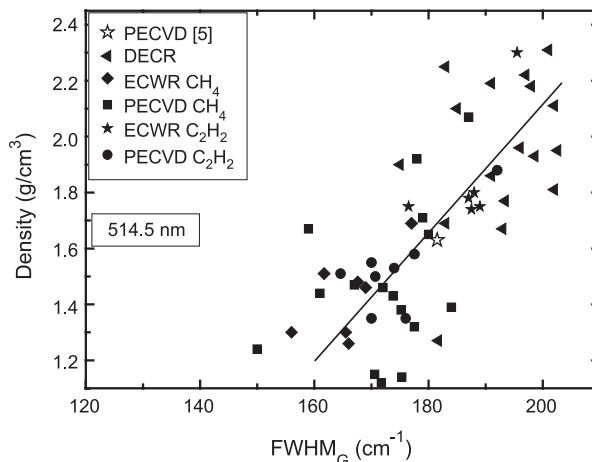
Fig. 3. Tauc gap as a function of H content.

Fig. 5. Density as a function of $FWHM_G$ measured at 514.5 nm.

Fig. 4a,b plots the Young's modulus and the density of the a-C:H films as a function of the $FWHM_G$ measured at 244 nm, for 20 at.%<H<50 at.%. A clear correlation is found, as was for hydrogen-free and nitrogenated carbon films [6,10,11]. Indeed, the density and mechanical properties of carbon films depend only on the C–C sp^3 content, and the $FWHM_G$ is proportional to the disorder of the carbon phase. By using the $FWHM_G$ at 514.5 nm, a similar trend is found (Fig. 5). However, for the 514.5-nm excitation, due to the PL background, the fit is less accurate, and the data spread is

bigger than at 244 nm. Furthermore, the 244-nm excitation is necessary in order to get a $FWHM_G$ even for high H content PLCH films, which do not show almost any measurable Raman peaks for 514.5 nm due to the very high PL background. On the other hand, a featureless visible Raman spectrum with no clear Raman peaks always indicates a low density (≤1.2 g/cm³) and low Young's modulus (≤20 GPa) PLCH.
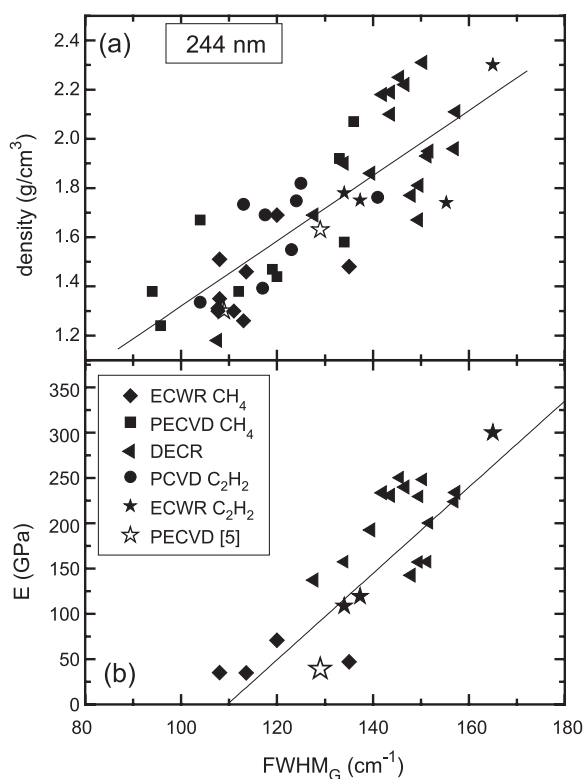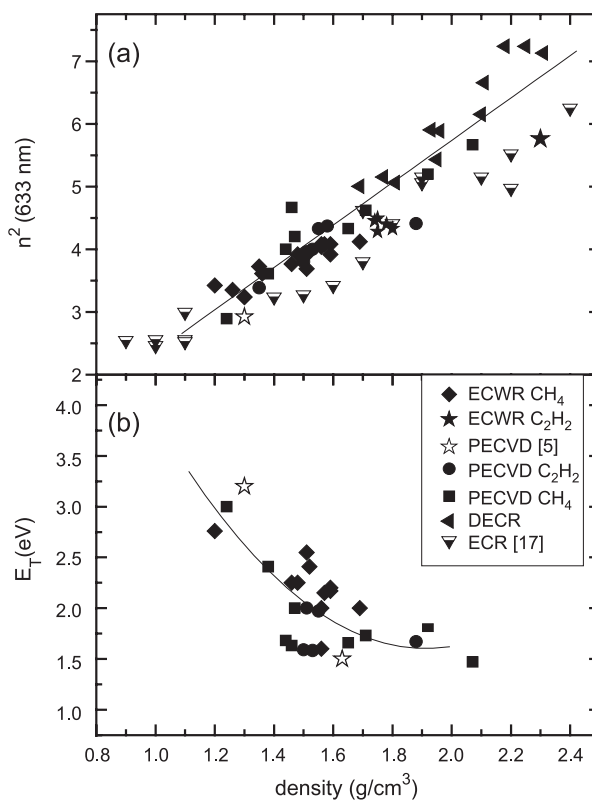

Fig. 4. (a) Density and (b) Young's modulus as a function of $FWHM_G$ measured at 244 nm.

Fig. 6. (a) Refractive index measured at 633 nm and (b) optical gap as a function of density.

From a linear fit of the data in Fig. 4a, we get the following simple relations:

$$\rho[\text{g/cm}^3] = 0.257 + 0.011 \times \text{FWHM}_G[\text{cm}^{-1}] \tag{3}$$

$$E[\text{GPa}] = -511 + 4.66\,\text{FWHM}_G[\text{cm}^{-1}] \tag{4}$$

The correlation of optical and mechanical properties in hydrogenated samples for 20 at.%<H<50 at.% is further demonstrated in Fig. 6, where the refractive index measured at 633 nm and the optical Gap are plotted as a function of the density. The fit of these data gives:

$$n^2 = -1 + 3.38 \times \rho[\text{g/cm}^3] \tag{5}$$

$$E_T[\text{eV}] = 8.87 - 6.85\rho[\text{g/cm}^3] + 1.54\rho^2[(\text{g/cm}^3)^2] \tag{6}$$

by combining Eqs. (2)–(6), we can get n and gap as a function of FWHM_G measured at 244 nm:

$$n^2 = -0.13 + 3.7 \times 10^{-2}\,\text{FWHM}_G[\text{cm}^{-1}] \tag{7}$$

$$E_T = 7.12 - 6.66 \cdot 10^{-2}\;\text{FWHM}_G[\text{cm}^{-1}] + 1.86 \cdot 10^{-4}$$
$$\times \text{FWHM}_{G^2}[(\text{cm}^{-1})^2] \tag{8}$$

These formulas are quite useful to get qualitative estimates from the Raman parameters, however they should be used with caution and carefully considering the possibility of exceptions and never for films with less than 20 at.% H. Indeed, graphs such as Figs. 3 and 6 must fail for H much lower than 20 at.%. This is easy to understand by considering the limiting cases of graphite and ta-C, both with 0 at.% H but with very different structural and optical properties. Furthermore, another reason of caution is that the optical properties depend on the sp^2 clustering. If in some conditions sp^2 clusters are produced independently of the H content, this will produce samples deviating from the simple trends shown so far. Again, clustering is very likely for low H content, but it is possible to find it also in high hydrogen samples. We will consider more in detail the case of clustering in another paper [13].

4. Conclusion

We presented a systematic analysis of the Raman spectra measured at 514.5 and 244 nm for a-C/H films, with H content between ~20% and 50%. All the relevant properties are to first approximation determined only by the H content.

Neglecting the cases when the sp^2 phase clustering can be independent from H content, we presented a set of simple correlation which allow to quickly estimate the structural and optical properties of a-C:Hs even by a single wavelength Raman measurement. Due to the increasing PL background with increasing H content, the best correlations are found for 244 nm measurements.

Acknowledgment

References

[1] J. Robertson, Mater. Sci. Eng., R Rep. 37 (2002) 129.
[2] A.C. Ferrari, A. Libassi, B.K. Tanner, V. Stolojan, J. Yuan, L.M. Brown, S.E. Rodil, B. Kleinsorge, J. Robertson, Phys. Rev., B 62 (2000) 11089.
[3] A.C. Ferrari, J. Robertson, M.G. Beghi, C.E. Bottani, R. Ferulano, R. Pastorelli, Appl. Phys. Lett. 75 (1999) 1893.
[4] N.A. Morrison, S.E. Rodil, A.C. Ferrari, J. Robertson, W.I. Milne, Thin Solid Films 337 (1999) 71.
[5] A.C. Ferrari, J. Robertson, Phys. Rev., B 61 (2000) 14095.
[6] A.C. Ferrari, J. Robertson, Phys. Rev., B 64 (2001) 075414.
[7] S. Piscanec, M. Lazzeri, F. Mauri, A.C. Ferrari, J. Robertson, Phys. Rev. Lett. 93 (2004) 185503.
[8] J. Robertson, Phys. Rev., B 53 (1996) 16302.
[9] B. Marchon, J. Gui, K. Grannen, G.C. Rauch, J.W. Ager III, S.R.P. Silva, J. Robertson, IEEE Trans. Magn. 33 (1997) 3148.
[10] A.C. Ferrari, S.E. Rodil, J. Robertson, Phys. Rev., B 67 (2003) 155306.
[11] C. Casiraghi, A.C. Ferrari, J. Robertson, R. Ohr, M.v. Gradowski, D. Schneider, Diamond Relat. Mater. 13 (2004) 1480.
[12] A.C. Ferrari, J. Roberson, Phys. Rev., B 63 (2001) 121405.
[13] C. Casiraghi, A.C. Ferrari, J. Robertson, J. Appl. Phys. (2004) (submitted for publication).
[14] A. Golanski, F. Piazza, J. Werckmann, G. Relihan, S. Schulze, J. Appl. Phys. 92 (2002) 3662.
[15] D. Schneider, T. Witke, T. Schwarz, B. Schoneich, B. Schultrich, Surf. Coat. Technol. 126 (2000) 136.
[16] M.A. Tamor, W.C. Vassell, J. Appl. Phys. 76 (1994) 3823.
[17] T. Schwarz-Sellinger, A. von Keudell, W. Jacob, J. Appl. Phys. 86 (1999) 3988.